

Detection of Fermi pairing via electromagnetically induced transparencyLei Jiang,¹ Han Pu,¹ Weiping Zhang,² and Hong Y. Ling³¹*Department of Physics and Astronomy, and Rice Quantum Institute, Rice University, Houston, Texas 77251, USA*²*State Key Laboratory of Precision Spectroscopy, Department of Physics, East China Normal University, Shanghai 200062, People's Republic of China*³*Department of Physics and Astronomy, Rowan University, Glassboro, New Jersey 08028-1700, USA*

(Received 9 March 2009; published 9 September 2009)

An optical spectroscopic method based on the principle of electromagnetically induced transparency (EIT) is proposed as quite a generic probing tool that provides valuable insights into the nature of Fermi pairing in ultracold Fermi gases of two hyperfine states. This technique has the capability of allowing spectroscopic response to be determined in a nearly nondestructive manner and the whole spectrum may be obtained by scanning the probe-laser frequency faster than the lifetime of the sample without re-preparing the atomic sample repeatedly. A quasiparticle picture is constructed to facilitate a simple physical explanation of the pairing signature in the EIT spectra.

DOI: [10.1103/PhysRevA.80.033606](https://doi.org/10.1103/PhysRevA.80.033606)

PACS number(s): 03.75.Ss, 05.30.Fk, 32.80.Qk

I. INTRODUCTION

The two-component degenerate Fermi gas, in which the interaction between atoms of two different hyperfine states is made magnetically tunable via Feshbach resonance, has been the main source of inspiration for much recent excitement at the forefront of ultracold atomic physics research. In addition to being an ideal system for the exploration of the crossover from a Bose-Einstein condensate (BEC) of highly localized pairs to nonlocal Bardeen-Cooper-Schrieffer (BCS) pairs, the degenerate Fermi gas, when operating in the unitarity regime, constitutes a strongly interacting Fermi gas exhibiting a rich set of physics, the study of which may shed light on long-standing problems in many different branches of physics, in particular, condensed-matter physics.

A unique phenomenon of low-temperature Fermi system is the formation of correlated Fermi pairs. How to detect pair formation in an indisputable fashion has remained a central problem in the study of ultracold atomic physics. Unlike the BEC transition of bosons for which the phase transition is accompanied by an easily detectable drastic change in atomic density profile, the onset of pairing in Fermi gases does not result in measurable changes in fermion density. Early proposals sought the BCS pairing signature from the images of off-resonance scattering light [1]. The underlying idea is that to gain pairing information, measurement must go beyond the first-order coherence, for example, to the density-density correlation. This is also the foundation for other detecting methods such as spatial noise correlations in the image of the expanding gas [2], Bragg scattering [3,4], Raman spectroscopy [5], Stokes-scattering method [6], radio frequency (RF) spectroscopy [7,8], optical detection of absorption [9], and interferometric method [10]. Among all these methods, RF spectroscopy [7,8] has been the only one implemented in current experiments [11,12].

In this paper, we propose an alternative detection scheme, whose principle of operation is illustrated in Fig. 1(a). In our scheme, a relatively strong coupling and a weak probe-laser field between the excited state $|e\rangle$ and, respectively, the ground state $|g\rangle$ and the spin-up state $|\uparrow\rangle$, form a Λ -type

energy diagram, which facilitates the use of the principle of electromagnetically induced transparency (EIT) to determine the nature of pairing in the interacting Fermi gas of two hyperfine spin states: $|\uparrow\rangle$ and $|\downarrow\rangle$. EIT [13], in which a probe-laser field experiences (virtually) no absorption but steep dispersion when operating around an atomic transition frequency, has been at the forefront of many exciting developments in the field of quantum optics [14]. Such a phenomenon is based on quantum interference, which is absent in measurement schemes such as in Ref. [6], where lasers are tuned far away from single-photon resonance. In the context of ultracold atoms, an important example is the experimental demonstration of dramatic reduction in light speed in the EIT medium in the form of Bose condensate [15]. This experiment has led to a renewed interest in EIT, motivated primarily at the prospect of the new possibilities that the slow speed and low intensity light may add to nonlinear optics [16] and quantum information processing [17]. More recently, EIT has been used to spectroscopically probe ultracold Rydberg atoms [18]. In this work, we will show how EIT can be exploited to reveal the nature of pairing in Fermi gases.

Before we present our detailed calculation, let us first compare the proposed EIT method with the RF spectroscopy method, which is widely used in probing Fermi gases nowadays. In the latter [7,8], an atomic sample is prepared and an RF pulse is applied to the sample, which couples one of the pairing states to a third atomic level $|3\rangle$. This is followed by a destructive measurement of the transferred atom numbers using absorption laser imaging. The RF signal is defined as the average rate change of the population in state $|3\rangle$ during the RF pulse, which can be inferred from the measured loss of atoms in $|\uparrow\rangle$. This process is repeated for another RF pulse with a different frequency. In addition to sparking many theoretical activities [19–23], this method has recently been expanded into the imbalanced Fermi gas systems [24–28], where pairing can result in a number of interesting phenomena [29]. A disadvantage of this method is its inefficiency: The sample must be prepared repeatedly for each RF pulse. In addition, for the most commonly used fermionic atom species, i.e., ${}^6\text{Li}$, the state $|3\rangle$ interacts strongly with the pair-

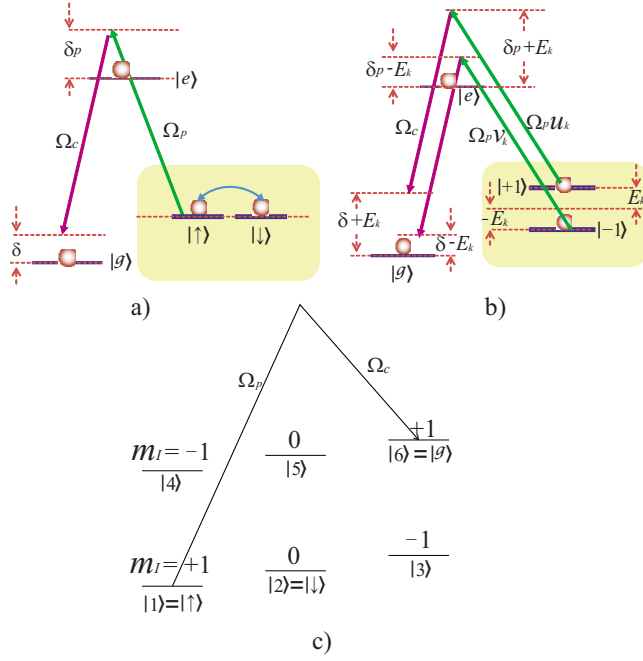


FIG. 1. (Color online) (a) The bare state picture of our model. (b) The dressed state picture of our model equivalent to (a). (c) A possible realization in ${}^6\text{Li}$. Here the states labeled by $|i\rangle$ ($i = 1, 2, \dots, 6$) are the six ground-state hyperfine states. Most experiments involving ${}^6\text{Li}$ are performed with a magnetic field strength tuned near a Feshbach resonance at 834G. Under such a magnetic field, the magnetic quantum number for the nuclear spin m_l is, to a very good approximation, a good quantum number. The values of m_l are shown in the level diagrams. Two-photon transition can only occur between states with the same m_l . Any pair of the lower manifold ($|1\rangle, |2\rangle$, and $|3\rangle$) can be chosen to form the pairing states. In the example shown here, we choose $|1\rangle = |\uparrow\rangle$, $|2\rangle = |\downarrow\rangle$, and $|6\rangle = |g\rangle$. The excited state $|e\rangle$ (not shown) can be chosen properly as one of the electronic p state.

ing states due to the fact that all three states involved has pairwise Feshbach resonances at relatively close magnetic field strength. This leads to so-called final-state effect [30], which greatly complicates the interpretation of the RF spectrum.

In the EIT method, by contrast, one can directly measure the absorption or transmission spectrum of the probe light. Applying a frequency scan faster than the lifetime of the atomic sample to the weak probe field, the whole spectrum can be recorded continuously in a nearly nondestructive fashion to the atomic sample. Furthermore, EIT signal results from quantum interference and is extremely sensitive to the two-photon resonance condition. The width of the EIT transparency window can be controlled by the coupling laser intensity and be made narrower than E_F . As we will show below, this property can be exploited to detect the onset of pairing as the pairing interaction shifts and destroys the two-photon resonance condition. In addition, due to different selection rules compared with the RF method, one can pick a different final state whose interaction with the pairing states are negligible [see Fig. 1(c)], hence avoiding the final-state effects.

The paper is organized as follows. In Sec. II, we described the model under study and define the key quantity of the proposal—the absorption coefficient of the probe light. In Sec. III, we present the expression of the probe absorption coefficient and construct a quasiparticle picture that will become convenient to explain the features of the spectrum. The results are presented in Sec. IV, where spectral features at different temperatures are explained. We also show that how EIT spectrum can be used to detect the onset of pairing. A brief summary is presented in Sec. V. Finally, we provide an Appendix where the derivation of the EIT spectrum is provided. In particular, we include in this derivation the pairing fluctuations in the framework of the pseudogap theory [19].

II. MODEL

Let us now describe our model in more detail, beginning with the definition of ω_i and Ω_i as the temporal and Rabi frequencies of the probe ($i=p$) and coupling ($i=c$) laser field of plane waves co-propagating with an almost identical wave vector \mathbf{k}_L (along z direction). The system to be considered is a homogeneous one with a total volume V , and can thus be described by operators $\hat{a}_{\mathbf{k},i}$ ($\hat{a}_{\mathbf{k},i}^\dagger$) for annihilating (creating) a fermionic atom in state $|i\rangle$ with momentum $\hbar\mathbf{k}$, and kinetic energy $\epsilon_k = \hbar^2 k^2 / 2m$, where m is the atomic mass. Here, $\hat{a}_{\mathbf{k},i}$ are defined in an interaction picture in which $\hat{a}_{\mathbf{k},e} = \hat{a}'_{\mathbf{k},e} e^{-i\omega_p t}$, $\hat{a}_{\mathbf{k},g} = \hat{a}'_{\mathbf{k},g} e^{i(\omega_c - \omega_p)t}$, and $\hat{a}_{\mathbf{k},\sigma} = \hat{a}'_{\mathbf{k},\sigma}$ ($\sigma = \uparrow, \downarrow$), where $\hat{a}'_{\mathbf{k},i}$ are the corresponding Schrödinger picture operators.

In a probe geometry, the signal to be measured is the probe-laser field, which is modified by a polarization having the same mathematical form as the probe field according to [31]

$$\frac{\partial \Omega_p}{\partial z} + \frac{1}{c} \frac{\partial \Omega_p}{\partial t} = i \frac{\mu_0 \omega_p c d_{e\uparrow}}{2} P_p \equiv \alpha \Omega_p, \quad (1)$$

where P_p is the slowly varying amplitude of that polarization, d_{ij} is the matrix element of the dipole moment operator between states $|i\rangle$ and $|j\rangle$, and μ_0 and c are the magnetic permeability and the speed of light in vacuum, respectively. The parameter α in Eq. (1) represents the complex absorption coefficient of the probe light [31]. By performing an ensemble average of atomic dipole moment, we can express α as

$$\alpha = i \frac{\alpha_0}{\Omega_p} \frac{1}{V} \sum_{\mathbf{k}, \mathbf{q}} \langle \hat{a}_{\mathbf{q},\uparrow}^\dagger \hat{a}_{\mathbf{k}+\mathbf{k}_L,e} \rangle e^{i(\mathbf{k}-\mathbf{q})\cdot\mathbf{r}}, \quad (2)$$

where $\alpha_0 \equiv \mu_0 \omega_p c |d_{e\uparrow}|^2$. The real and imaginary parts of α correspond to the probe absorption and dispersion spectrum, respectively.

To determine the probe spectrum, we start from the grand canonical Hamiltonian $\hat{H} = \sum_{\mathbf{k}} (\hat{\mathcal{H}}_{1\mathbf{k}} + \hat{\mathcal{H}}_{2\mathbf{k}} + \hat{\mathcal{H}}_{3\mathbf{k}})$, where

$$\hat{\mathcal{H}}_{1\mathbf{k}} = (\epsilon'_k - \delta_p) \hat{a}_{\mathbf{k},e}^\dagger \hat{a}_{\mathbf{k},e} + (\epsilon'_k - \delta) \hat{a}_{\mathbf{k},g}^\dagger \hat{a}_{\mathbf{k},g},$$

$$\hat{\mathcal{H}}_{2\mathbf{k}} = -\frac{1}{2} (\Omega_c \hat{a}_{\mathbf{k}+\mathbf{k}_L,e}^\dagger \hat{a}_{\mathbf{k},g} + \Omega_p \hat{a}_{\mathbf{k}+\mathbf{k}_L,e}^\dagger \hat{a}_{\mathbf{k},\uparrow}) - \text{H.c.},$$

$$\hat{H}_{3\mathbf{k}} = \sum_{\sigma} \epsilon'_k \hat{a}_{\mathbf{k},\sigma}^{\dagger} \hat{a}_{\mathbf{k},\sigma} - (\Delta \hat{a}_{\mathbf{k},\uparrow}^{\dagger} \hat{a}_{-\mathbf{k},\downarrow}^{\dagger} + \text{H.c.})$$

describe the bare atomic energies of states $|e\rangle$ and $|g\rangle$, the dipole interaction between atoms and laser fields, and the mean-field Hamiltonian for the spin-up and -down subsystems, respectively. Here, $\epsilon'_k = \epsilon_k - \mu$ with μ being the chemical potential, $\delta_p = \hbar(\omega_p - \omega_{e\uparrow})$ and $\delta_c = \hbar(\omega_c - \omega_{eg})$ are the single-photon detunings, and $\delta = \delta_p - \delta_c$ is the two-photon detuning with ω_{ij} being the atomic transition frequency from level $|i\rangle$ to $|j\rangle$. In arriving at $\hat{H}_{3\mathbf{k}}$, in order for the main physics to be most easily identified, we have expressed the collisions between atoms of opposite spins in terms of the gap parameter $\Delta = -UV^{-1} \sum_{\mathbf{k}} \langle \hat{a}_{-\mathbf{k},\downarrow} \hat{a}_{\mathbf{k},\uparrow} \rangle$ under the assumption of BCS pairing, where U characterizes the interaction between $|\uparrow\rangle$ and $|\downarrow\rangle$ which, in the calculation, will be replaced in favor of the s -wave scattering length a_s via the regularization procedure,

$$\frac{m}{4\pi\hbar^2 a_s} = \frac{1}{U} + \frac{1}{V} \sum_{\mathbf{k}} \frac{1}{2\epsilon_k}.$$

A more complex model including the pseudogap physics [19] will be presented later in the paper. Finally, we note that the effect of the collisions involving the final state $|g\rangle$ in the RF spectrum has been a topic of much recent discussion [21–23]. In our model, the spectra are not limited to the RF regime, and this may provide us with more freedom to choose $|g\rangle$ (and $|e\rangle$) that minimizes the final-state effect. In what follows, for the sake of simplicity, we ignore the collisions involving states $|g\rangle$ (and $|e\rangle$). In practice, the effects of final-state interaction can be minimized by choosing the proper atomic species [32] or hyperfine spin states [30]. In the example shown in Fig. 1(c), it is indeed expected that $|g\rangle$ does not interact strongly with either of the pairing state.

III. QUASIPARTICLE PICTURE

The part of the Hamiltonian describing the pairing of the fermions can be diagonalized using the standard Bogoliubov transformation,

$$\hat{a}_{\mathbf{k},\uparrow} = u_k \hat{\alpha}_{\mathbf{k},\uparrow} + v_k \hat{\alpha}_{-\mathbf{k},\downarrow}^{\dagger},$$

$$\hat{a}_{-\mathbf{k},\downarrow}^{\dagger} = -v_k \hat{\alpha}_{\mathbf{k},\uparrow} + u_k \hat{\alpha}_{-\mathbf{k},\downarrow}^{\dagger},$$

where $u_k = \sqrt{(E_k + \epsilon'_k)/2E_k}$, $v_k = \sqrt{(E_k - \epsilon'_k)/2E_k}$, and $E_k = \sqrt{\epsilon_k'^2 + \Delta^2}$ is the quasiparticle energy dispersion. Now we introduce two sets of quasiparticle states $|\pm 1_{\mathbf{k}}\rangle$, representing the electron and hole branches, respectively. The corresponding field operators are defined as

$$\hat{\alpha}_{\mathbf{k},+1} \equiv \hat{\alpha}_{\mathbf{k},\uparrow}, \quad \hat{\alpha}_{\mathbf{k},-1} \equiv \hat{\alpha}_{-\mathbf{k},\downarrow}^{\dagger},$$

in terms of which, the grand canonical Hamiltonian can be written as

$$\begin{aligned} \hat{H} = \sum_{\mathbf{k}} \left[& (\epsilon'_k - \delta_p) \hat{a}_{\mathbf{k},e}^{\dagger} \hat{a}_{\mathbf{k},e} + (\epsilon'_k - \delta) \hat{a}_{\mathbf{k},g}^{\dagger} \hat{a}_{\mathbf{k},g} + E_k \hat{\alpha}_{\mathbf{k},+1}^{\dagger} \hat{\alpha}_{\mathbf{k},+1} \right. \\ & - E_k \hat{\alpha}_{\mathbf{k},-1}^{\dagger} \hat{\alpha}_{\mathbf{k},-1} - \left. \left(\frac{\Omega_c}{2} \hat{a}_{\mathbf{k}+\mathbf{k}_L,e}^{\dagger} \hat{a}_{\mathbf{k},g} + \text{H.c.} \right) \right. \\ & - \left. \left(\frac{\Omega_p u_k}{2} \hat{a}_{\mathbf{k}+\mathbf{k}_L,e}^{\dagger} \hat{\alpha}_{\mathbf{k},+1} + \text{H.c.} \right) \right. \\ & \left. - \left(\frac{\Omega_p v_k}{2} \hat{a}_{\mathbf{k}+\mathbf{k}_L,e}^{\dagger} \hat{\alpha}_{\mathbf{k},-1} + \text{H.c.} \right) \right]. \end{aligned} \quad (3)$$

A physical picture emerges from this Hamiltonian very nicely. The state $|+1_{\mathbf{k}}\rangle$ ($|-1_{\mathbf{k}}\rangle$) has an energy dispersion $+E_k$ ($-E_k$) and is coupled to the excited state $|e\rangle$ by an effective Rabi frequency $\Omega_p u_k$ ($\Omega_p v_k$), which is now a function of k . In the quasiparticle picture, our model becomes a double Λ system as illustrated in Fig. 1(b). Let $+\Lambda$ ($-\Lambda$) denote the Λ configuration involving $|+1_{\mathbf{k}}\rangle$ ($|-1_{\mathbf{k}}\rangle$). The $+\Lambda$ ($-\Lambda$) system is characterized with a single-photon detuning of $\delta_p + E_k$ ($\delta_p - E_k$) and a two-photon detuning of $\delta + E_k$ ($\delta - E_k$). In thermal equilibrium at temperature T (in the absence of the probe field), we have

$$\langle \hat{\alpha}_{\mathbf{k},+1}^{\dagger} \hat{\alpha}_{\mathbf{k}',+1} \rangle = \delta_{\mathbf{k},\mathbf{k}'} - \langle \hat{\alpha}_{\mathbf{k},-1}^{\dagger} \hat{\alpha}_{\mathbf{k}',-1} \rangle = \delta_{\mathbf{k},\mathbf{k}'} f(E_k), \quad (4)$$

where

$$f(\omega) = [\exp(\omega/k_B T) + 1]^{-1} \quad (5)$$

is the standard Fermi-Dirac distribution for quasiparticles. Thus, as temperature increases from zero, the probability of finding a quasiparticle in state $|+1_{\mathbf{k}}\rangle$ increases, while that in state $|-1_{\mathbf{k}}\rangle$ decreases but the total probability within each momentum group remains unchanged. Similarly, in the quasiparticle picture, the probe spectrum receives contributions from two transitions

$$\begin{aligned} \alpha = i \frac{\alpha_0}{\Omega_p} \frac{1}{V} \sum_{\mathbf{k},\mathbf{q}} e^{i(\mathbf{k}-\mathbf{q})\cdot\mathbf{r}} \\ \times [u_q \rho_{e,+1}(\mathbf{k} + \mathbf{k}_L, \mathbf{q}) + v_q \rho_{e,-1}(\mathbf{k} + \mathbf{k}_L, \mathbf{q})], \end{aligned} \quad (6)$$

where $\rho_{i,\pm 1}(\mathbf{k}, \mathbf{k}') = \langle \hat{\alpha}_{\mathbf{k}',\pm 1}^{\dagger} \hat{\alpha}_{\mathbf{k},i} \rangle$ are the off-diagonal density-matrix elements in momentum space.

The equations for the density-matrix elements can be obtained by averaging, with respect to the thermal equilibrium defined in Eq. (4), the corresponding Heisenberg's equations of motion based upon Hamiltonian (3). In the regime where the linear-response theory holds, the terms at the second order and higher can be ignored, and the density-matrix elements correct up to the first order in Ω_p are then found to be governed by the following coupled equations:

$$\begin{aligned} i\hbar \frac{d}{dt} \begin{bmatrix} \rho_{e,\eta}(\mathbf{k} + \mathbf{k}_L, \mathbf{q}) \\ \rho_{g,\eta}(\mathbf{k}, \mathbf{q}) \end{bmatrix} \\ = M_{\eta} \begin{bmatrix} \rho_{e,\eta}(\mathbf{k} + \mathbf{k}_L, \mathbf{q}) \\ \rho_{g,\eta}(\mathbf{k}, \mathbf{q}) \end{bmatrix} - \frac{\Omega_p}{2} \Lambda_{\eta}(\mathbf{k}) \delta_{\mathbf{k},\mathbf{q}} (\eta = \pm 1), \end{aligned} \quad (7)$$

where

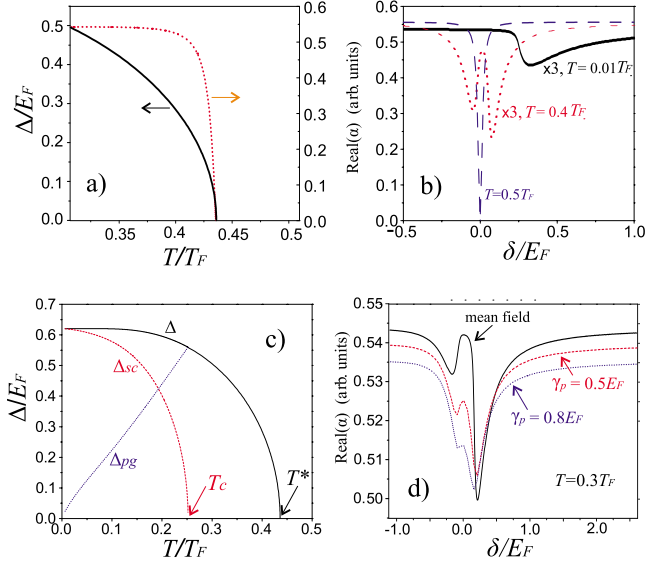


FIG. 2. (Color online) (a) Δ (black solid curve) and the probe absorption coefficient real(α) at $\delta=0$ (red dotted curve) as functions of T , obtained from the mean-field BCS theory. (b) Real(α) as a function of δ (absorption spectrum) at different T . (c) Δ , Δ_{sc} , and Δ_{pg} as functions of T obtained from the pseudogap approach. ($\Delta_{sc}=0$ and $\Delta=\Delta_{pg}$ when $T_c < T < T^*$). (d) A comparison of various absorption spectra at $T=0.3T_F$. The parameters are $\delta_c=0$, $\gamma=380E_F$ (~ 10 MHz), $\Omega_c=5E_F$ (~ 0.1 MHz), and $1/(k_F a_s)=-0.1$.

$$\Lambda_{+1}(\mathbf{k}) = \begin{pmatrix} u_k f(E_k) \\ 0 \end{pmatrix}, \Lambda_{-1}(\mathbf{k}) = \begin{pmatrix} v_k f(-E_k) \\ 0 \end{pmatrix}$$

and

$$M_\eta = \begin{bmatrix} \epsilon'_k - \delta_p - \eta E_k - i\gamma & -\frac{\Omega_c}{2} \\ -\frac{\Omega_c^*}{2} & \epsilon'_k - \delta - \eta E_k \end{bmatrix}.$$

Here we have introduced phenomenologically the parameter γ , which represents the decay rate of the excited state $|e\rangle$. Inserting the steady-state solution from Eq. (7) into Eq. (6), we immediately arrive at $\alpha(\delta_c, \delta) = \alpha_{+1}(\delta_c, \delta) + \alpha_{-1}(\delta_c, \delta)$, where

$$\alpha_{\pm 1}(\delta_c, \delta) = i \frac{\alpha_0}{2V} \sum_{\mathbf{k}} w_{\mathbf{k}}(\delta_c, \delta, \pm E_k) f(\pm E_k) \begin{cases} u_k^2 \\ v_k^2 \end{cases}, \quad (8)$$

with

$$w_{\mathbf{k}}(\delta_c, \delta, \omega) = \frac{\epsilon'_k - \delta - \omega}{\lambda_{\mathbf{k}}(\delta_c, \delta, \omega)(\epsilon'_k - \delta - \omega) - |\Omega_c/2|^2}, \quad (9)$$

$$\text{and } \lambda_{\mathbf{k}}(\delta_c, \delta, \omega) = \epsilon'_{\mathbf{k}+\mathbf{k}_L} - \delta_c - \delta - i\gamma - \omega.$$

IV. RESULTS

Examples of the probe absorption coefficient, $\text{Re}(\alpha)$, are presented in Figs. 2(a) and 2(b). For the results shown in this paper, we choose $1/(k_F a_s) = -0.1$, where we denote E_F , k_F ,

and $T_F = E_F/k_B$ be Fermi energy, wave number, and temperature, respectively, for the noninteracting Fermi gas. The black solid line in Fig. 2(a) represents the gap parameter in the mean-field calculation, from which we can see that the critical temperature below which the system exhibits pairing is given by $T_c = 0.435T_F$ for the parameters chosen. The dotted red curve in Fig. 2(a) represents the absorption coefficient at two-photon resonance $\delta=0$. We can see that it remains at zero for $T > T_c$ but increases sharply once the temperature drops below T_c . We note that this feature can be used as a sensitive gauge for detecting the onset of Fermi pairing. With this being emphasized, we now turn to explain the main spectroscopic features displayed in Fig. 2(b).

First, as long as $T > T_c$ where $\Delta=0$, one can show that the spectrum is essentially independent of T and

$$\text{Re}(\alpha) \propto \frac{\delta^2}{[(\delta + \delta_c)\delta - |\Omega_c/2|^2]^2 + \delta^2 \gamma^2}.$$

From this expression, one can easily see that there exists around $\delta=0$ a narrow transparency window with a width determined by the optical pumping rate $\Gamma_{op} = |\Omega_c|^2 \gamma / [4(\delta_c^2 + \gamma^2)]$ [see the blue dashed curve for $T=0.5T_F$ in Fig. 2(b)]. This feature can be most easily understood from the bare state picture [Fig. 1(a)], where state $|\uparrow\rangle$ is decoupled from state $|\downarrow\rangle$ so that the spectrum is of EIT type for a Λ system involving $|e\rangle$, $|g\rangle$, and $|\uparrow\rangle$. Further, because states $|g\rangle$ and $|\uparrow\rangle$ share the same energy dispersion ϵ'_k , the two-photon resonance condition $\delta=0$ holds for atoms of any velocity groups; the absence of absorption at $\delta=0$ signals the existence of a coherent population trapping state.

As T decreases below T_c , a double-peak structure develops [see the red dotted line for $T=0.4T_F$ in Fig. 2(b)]. The two peaks can be understood as contributed by the quasiparticle state $|+1_{\mathbf{k}}\rangle$ and $|-1_{\mathbf{k}}\rangle$, respectively. In the limit where T is far below T_c [see the black solid line for $T=0.01T_F$ in Fig. 2(b)], $+1_{\mathbf{k}}$ system has negligible contribution to the probe spectrum because there exists virtually no quasiparticles in state $|+1_{\mathbf{k}}\rangle$. Thus, the spectrum is solely contributed by $-1_{\mathbf{k}}$ system, resulting in a single-peak structure. However, unlike the situations above T_c , here while the dispersion of an atom in state $|g\rangle$ continues to be ϵ'_k , the dispersion of a dressed particle in state $|-1_{\mathbf{k}}\rangle$ is $-E_k$. As a result, the effective two-photon resonance condition $\epsilon'_k - \delta + E_k = 0$ is now momentum dependent. Aside from a shift, the transparency window becomes inhomogeneously broadened with a linewidth in the order of E_F . A consequence of the momentum dependence of the two-photon resonance condition is that, for any given probe-laser frequency, only atoms with the “right” momentum result in perfect destructive quantum interference. Consequently, $\text{Re}(\alpha)$ can no longer be zero for any probe frequency. This underlies the sharp increase in the probe absorption at $\delta=0$ below T_c as shown in Fig. 2(a).

We also want to emphasize that the spectrum shown in Fig. 2(b) can be obtained by scanning the probe-laser frequency over a range on the order of $E_F \sim 0.1$ MHz. We may take typical spectral features of the Fermi gas to be $\delta\omega \sim 0.1E_F \sim 10$ KHz. To resolve such features, using the energy-time uncertainty relation, we can use a scan rate of

10KHz/0.1ms, then the total scan time can be estimated to be around 1 ms. As this time is much shorter compared with the typical lifetime of the Fermi gas, this method can be regarded as nearly nondestructive. This demonstrates the great efficiency of the EIT probe.

In a more realistic model where pair fluctuations are included, gap Δ is divided into a BCS gap Δ_{sc} for condensed (BCS) pairs below T_c and a pseudogap Δ_{pg} for preformed (finite momentum) pairs below temperature T^* according to $\Delta^2 = \Delta_{sc}^2 + \Delta_{pg}^2$ [19]. Results including pseudogap physics are illustrated in Figs. 2(c) and 2(d) and the detailed derivations can be found in the Appendix. In contrast to the weakly interacting regime, where T^* is virtually the same as T_c , T^* is much higher than T_c in strongly interacting regime as is clearly the case of present study according to Fig. 2(c). It needs to be stressed that pair fluctuations can result in a finite lifetime γ_p^{-1} for preformed pairs which tend to broaden the spectral features, so that only when γ_p is sufficiently small can the double-peak spectroscopic structure be resolved as Fig. 2(d) demonstrates. Finally, the two-photon resonance here is only sensitive to Δ because E_k depends on the total gap Δ [19]. As a result, like its RF counterpart [24], the EIT method cannot distinguish between Δ_{sc} and Δ_{pg} . However, the qualitative features of Fig. 2(a) are not changed as long as we regard the corresponding critical temperature as T^* .

V. SUMMARY

In summary, we propose to use optical spectroscopy in an EIT setting to probe the fermionic pairing in Fermi gases. We have demonstrated that the EIT technique offers an extremely efficient probing method and is capable of detecting the onset of pair formation (i.e., determining T^*) due to its spectral sensitivity. With a sufficiently weak probe field, the whole spectrum may be obtained with a nearly nondestructive fashion via a relatively fast scan of probe frequency, without the need of repeatedly re-preparing the sample. We note that in this work, we have focused on probing the atomic system using photons. In the future, it will also be interesting to study how we can use atomic Fermi gas to manipulate the light. Superfluid fermions can serve a new type of nonlinear media for photons. Finally, we want to remark that, in this work, as a proof of principle, we have only considered a homogeneous system. As usual, the trap inhomogeneity can be easily accounted for within local-density approximation. Nevertheless, we note that the capability of detecting the onset of pairing remains the same even in the presence of the trap. Furthermore, as optical fields are used in this scheme, one may focus the probe-laser beam such that only a small localized portion of the atomic cloud is probed, hence there is no need to average over the whole cloud.

ACKNOWLEDGMENTS

We thank Randy Hulet for insightful discussions. This work is supported by the U.S. National Science Foundation (H.P. and H.Y.L.), the U.S. Army Research Office (H.Y.L.), the Robert A. Welch Foundation (Grant No. C-1669), the

W. M. Keck Foundation (L.J. and H.P.), the National Natural Science Foundation of China (Grant No. 10588402), the National Basic Research Program of China (973 Program) (Grant No. 2006CB921104), the Program of Shanghai Subject Chief Scientist (Grant No. 08XD14017), and the Program for Changjiang Scholars and Innovative Research Team in University, Shanghai Leading Academic Discipline Project (Grant No. B480) (W.Z.).

APPENDIX: EIT SPECTRA INCLUDING PSEUDOGAP

In this appendix, we generalize the result of Eq. (2) for α valid under the mean-field BCS pairing to a more realistic situation where pair fluctuations are included in the form of pseudogap. We show two different ways to accomplish this generalization. The first is an approach used more often by people working in the field of quantum optics. The second uses the linear-response theory [33] more familiar in the field of condensed-matter physics.

1. Brief account of pseudogap theory

First, let us highlight the results of pseudogap theory [19] that are relevant to our EIT spectrum calculation. When pairing fluctuations at finite temperature are included in the framework of the pseudogap model [19], the BCS gap equation and number equation are still valid. However, the gap Δ is now regarded as the total gap divided into a BCS gap Δ_{sc} for condensed (BCS) pairs below T_c and a pseudogap Δ_{pg} for preformed (finite momentum) pairs,

$$\Delta^2 = \Delta_{sc}^2 + \Delta_{pg}^2.$$

The onset of the total gap Δ occurs at temperature T^* , which is greater than T_c . The system with preformed pairs is described by the Green's function

$$G^{-1}(\mathbf{k}, iw_n) = G_0^{-1}(\mathbf{k}, iw_n) - \Sigma(\mathbf{k}, iw_n), \quad (\text{A.1})$$

where the noninteracting Green's function

$$G_0(\mathbf{k}, iw_n) = (iw_n - \epsilon'_k)^{-1}, \quad (\text{A.2})$$

and the self-energy

$$\begin{aligned} \Sigma(\mathbf{k}, iw_n) &= \Sigma_{sc}(\mathbf{k}, iw_n) + \Sigma_{pg}(\mathbf{k}, iw_n) \\ &= \frac{\Delta_{sc}^2}{iw_n + \epsilon'_k} + \frac{\Delta_{pg}^2}{iw_n + \epsilon'_k + i\gamma_p}, \end{aligned} \quad (\text{A.3})$$

with w_n being the Fermi Matsubara frequency and γ_p^{-1} the finite lifetime of pseudogap pairs. The spectral function $A(\mathbf{k}, \omega)$ can be obtained from the Green's function via the relation

$$A(\mathbf{k}, \omega) = -2 \text{Im} G(\mathbf{k}, \omega + i0^+),$$

which, with the help of Eqs. (A.1)–(A.3), is found to be given by

$$A(\mathbf{k}, \omega) = \frac{2(\omega + \epsilon'_k)^2 \gamma_p \Delta_{pg}^2}{[\omega^2 - E_k^2]^2 (\omega + \epsilon'_k)^2 + \gamma_p^2 [\omega^2 - E_k^{sc2}]^2}, \quad (\text{A.4})$$

where $E_k^{sc} = \sqrt{\epsilon_k'^2 + \Delta_{sc}^2}$. In the limit of $\gamma_p \rightarrow 0$ and $E_k^{sc} \rightarrow E_k$, we recover from Eq. (A.4) the spectral function under the BCS paring

$$A(\mathbf{k}, \omega) = 2\pi[u_k^2 \delta(\omega - E_k) + v_k^2 \delta(\omega + E_k)]. \quad (\text{A.5})$$

2. Quantum optics approach

In order to develop a formalism which directly incorporates the spectral function, we rewrite Eq. (8) in terms of the equal-time correlation function $h_{\mathbf{q},\mathbf{k}}(t) = \langle \hat{a}_{\mathbf{q},\uparrow}^\dagger(t) \hat{a}_{\mathbf{k}+\mathbf{k}_L,e}(t) \rangle$ as

$$\alpha = i \frac{\alpha_0}{\Omega_p} \frac{1}{V} \lim_{t \rightarrow \infty} \sum_{\mathbf{k}, \mathbf{q}} h_{\mathbf{q},\mathbf{k}}(t) e^{i(\mathbf{k}-\mathbf{q}) \cdot \mathbf{r}}, \quad (\text{A.6})$$

where the limit is introduced to indicate explicitly that we are interested in the steady-state spectrum. Here, $\hat{a}_{\mathbf{q},\uparrow}^\dagger(t)$ and $\hat{a}_{\mathbf{k}+\mathbf{k}_L,e}(t)$ obey the Heisenberg equations of motion

$$i\hbar \frac{d}{dt} \begin{pmatrix} \hat{a}_{\mathbf{k}+\mathbf{k}_L,e} \\ \hat{a}_{\mathbf{k},g} \end{pmatrix} = \hat{M} \begin{pmatrix} \hat{a}_{\mathbf{k}+\mathbf{k}_L,e} \\ \hat{a}_{\mathbf{k},g} \end{pmatrix} - \frac{\Omega_p}{2} \hat{a}_{\mathbf{k},\uparrow} \begin{pmatrix} 1 \\ 0 \end{pmatrix}, \quad (\text{A.7})$$

with

$$\hat{M} = \begin{bmatrix} \epsilon'_{\mathbf{k}+\mathbf{k}_L} - (\delta_p + i\gamma) & -\frac{\Omega_c}{2} \\ -\frac{\Omega_c^*}{2} & \epsilon'_k - \delta \end{bmatrix}. \quad (\text{A.8})$$

Note that due to the dissipative nature of our model, strictly speaking, Eqs. (A.7) should be those of quantum Langevin equations containing the noise operators of the reservoir that gives rise to the decay rate γ . Here, in anticipation that Eqs. (A.7) will produce the right averages of our interest, we have ignored the noise operators. We solve Eqs. (A.7) for $\hat{a}_{\mathbf{k}+\mathbf{k}_L,e}(t)$ in the limit of $t \rightarrow \infty$ when the terms involving the initial operators have all died away, and then combine it with $\hat{a}_{\mathbf{q},\uparrow}^\dagger(t)$ to form

$$h_{\mathbf{q},\mathbf{k}}(t) = \frac{\Omega_p}{2} \int_0^t [e^{-i\hat{M}(t-t')}]_{11} G^<(\mathbf{k}, t', t) \delta_{\mathbf{k},\mathbf{q}} dt', \quad (\text{A.9})$$

where $[\dots]_{11}$ denotes the element at the first row and the first column of the matrix inside the square bracket, and $G^<(\mathbf{k}, t', t) = i \langle \hat{a}_{\mathbf{k},\uparrow}^\dagger(t) \hat{a}_{\mathbf{k},\uparrow}(t') \rangle$ is one of the Green's functions in real time. By substituting $G^<(\mathbf{k}, t', t)$ in Eq. (A.9) with a Fourier transformation of its counterpart in real frequency, $G^<(\mathbf{k}, \omega)$, we are able to carry out the time integration in Eq. (A.9) explicitly, leading to

$$h_{\mathbf{q},\mathbf{k}}(t \rightarrow \infty) = \delta_{\mathbf{k},\mathbf{q}} \frac{\Omega_p}{2} \int_{-\infty}^{+\infty} \frac{d\omega}{2\pi} \left[\frac{A(\mathbf{k}, \omega) f(\omega)}{\hat{M} - \omega} \right]_{11},$$

where the use of a well-known relation: $G^<(\mathbf{k}, \omega) = \text{if}(\omega) A(\mathbf{k}, \omega)$ [33] has been made. Finally, replacing $[1/(\hat{M} - \omega)]_{11}$ with $w_{\mathbf{k}}(\delta_c, \delta, \omega)$, obtained with the help of Eq. (A.8), we arrive at

$$\alpha = i \frac{\alpha_0}{2V} \sum_{\mathbf{k}} \int_{-\infty}^{+\infty} \frac{d\omega}{2\pi} A(\mathbf{k}, \omega) f(\omega) w_{\mathbf{k}}(\delta_c, \delta, \omega), \quad (\text{A.10})$$

where $w_{\mathbf{k}}(\delta_c, \delta, \omega)$ is defined in Eq. (9) of the main text. One can easily check that Eq. (A.10) reduces to Eq. (8) in the

limit of mean-field BCS pairing when Eq. (A.5) is used as the spectral function.

3. Condensed matter approach

In order to use the linear-response theory widely used in condensed-matter physics, we first divide our system into a ‘‘left part’’ comprising two hyperfine spin states: $|\uparrow\rangle$ and $|\downarrow\rangle$, whose physics has been described in Appendix, Sec. 1, a ‘‘right part’’ consisting of the coupling laser field and states $|g\rangle$ and $|e\rangle$, described by the Hamiltonian

$$\hat{H}_R = \sum_{\mathbf{k}} [(\epsilon'_k - \delta_p) \hat{a}_{\mathbf{k},e}^\dagger \hat{a}_{\mathbf{k},e} + (\epsilon'_k - \delta) \hat{a}_{\mathbf{k},g}^\dagger \hat{a}_{\mathbf{k},g}] - \left(\frac{\Omega_c}{2} \sum_{\mathbf{k}} \hat{a}_{\mathbf{k}+\mathbf{k}_L,e}^\dagger \hat{a}_{\mathbf{k},g} + \text{H.c.} \right),$$

and finally the coupling between the two parts induced by the probe field, described by the tunneling Hamiltonian

$$\hat{H}_T = -\frac{\Omega_p}{2} \sum_{\mathbf{k}} \hat{a}_{\mathbf{k}+\mathbf{k}_L,e}^\dagger \hat{a}_{\mathbf{k},\uparrow} + \text{H.c.} \equiv \hat{A} + \hat{A}^\dagger.$$

Next, we change H_R into a diagonal form

$$H_R = \sum_{\mathbf{k}} [E_k^\alpha \hat{\alpha}_{\mathbf{k}}^\dagger \hat{\alpha}_{\mathbf{k}} + E_k^\beta \hat{\beta}_{\mathbf{k}}^\dagger \hat{\beta}_{\mathbf{k}}], \quad (\text{A.11})$$

in terms of a pair of dressed state operators, $\hat{\alpha}$ and $\hat{\beta}$, defined via the transformation

$$\begin{bmatrix} \hat{a}_{\mathbf{k}+\mathbf{k}_L,e} \\ \hat{a}_{\mathbf{k},g} \end{bmatrix} = \begin{bmatrix} u_k^\alpha & u_k^\beta \\ v_k^\alpha & v_k^\beta \end{bmatrix} \begin{bmatrix} \hat{\alpha}_{\mathbf{k}} \\ \hat{\beta}_{\mathbf{k}} \end{bmatrix}, \quad (\text{A.12})$$

where

$$(u_k^{\alpha,\beta})^2 = (v_k^{\beta,\alpha})^2 = \frac{1}{2} \left(1 \pm \frac{\zeta_k - \eta_k}{\sqrt{(\zeta_k - \eta_k)^2 + |\Omega_c|^2}} \right), \quad (\text{A.13})$$

$$E_k^{\alpha,\beta} = \frac{1}{2} (\zeta_k + \eta_k \pm \sqrt{(\zeta_k - \eta_k)^2 + |\Omega_c|^2}), \quad (\text{A.14})$$

with $\zeta_k = \epsilon'_{\mathbf{k}+\mathbf{k}_L} - \delta_p$ and $\eta_k = \epsilon'_k - \delta$. In terms of the dressed state operators, \hat{A} becomes

$$\hat{A} = -\frac{\Omega_p}{2} \sum_{\mathbf{k}} [u_k^\alpha \hat{\alpha}_{\mathbf{k}}^\dagger \hat{a}_{\mathbf{k},\uparrow} + u_k^\beta \hat{\beta}_{\mathbf{k}}^\dagger \hat{a}_{\mathbf{k},\uparrow}] \quad (\text{A.15})$$

and is in a form to which the linear-response theory [33] is directly applicable. Following the standard practice, we then find

$$\langle \hat{A} \rangle = \frac{\Omega_p^2}{4} \sum_{\mathbf{k}} \sum_{\eta=\alpha,\beta} (u_k^\eta)^2 \int_{-\infty}^{+\infty} \frac{d\omega_L}{2\pi} A_L(\mathbf{k}, \omega_L) \times \int_{-\infty}^{+\infty} \frac{d\omega_R}{2\pi} A_R^\eta(\mathbf{k}, \omega_R) \frac{f(\omega_R) - f(\omega_L)}{\omega_R - \omega_L + i0^+}. \quad (\text{A.16})$$

In Eq. (A.16), $A_L(\mathbf{k}, \omega_L)$ is same as $A(\mathbf{k}, \omega_L)$ defined in Eq. (A.4), while $A_R^\eta(\mathbf{k}, \omega_R)$ is given by $2\pi\delta(\omega_R - E_k^\eta)$ because the right part is in a normal state described by the Green's function $G_\eta^{-1}(\mathbf{k}, i\omega_n) = i\omega_n - E_k^\eta$. Integrating over ω_R , we change Eq. (A.16) into

$$\langle \hat{A} \rangle = \frac{\Omega_p^2}{4} \sum_{\mathbf{k}} \sum_{\eta=\alpha,\beta} (u_k^\eta)^2 \int_{-\infty}^{+\infty} \frac{d\omega}{2\pi} A(\mathbf{k}, \omega) \frac{f(E_k^\eta) - f(\omega)}{E_k^\eta - \omega + i0^+}, \quad (\text{A.17})$$

where the dummy variable ω_L has been changed into ω . We now include the effect of the decay of the excited state phenomenologically by replacing δ_p with $\delta_p - i\gamma$. We see that E_k^η

now become imaginary, which signals the inability of the dressed states to hold populations. This along with the fact that the dressed states here are the superpositions of the initially empty states provides us with the justification to set $f(E_k^\eta) = 0$ in Eq. (A.17). With these considerations, we finally arrive at

$$\langle \hat{A} \rangle = -\frac{\Omega_p^2}{4} \sum_{\mathbf{k}} \int_{-\infty}^{+\infty} \frac{d\omega}{2\pi} A(\mathbf{k}, \omega) f(\omega) w_{\mathbf{k}}(\delta_c, \delta, \omega), \quad (\text{A.18})$$

where the use of Eqs. (A.13) and (A.14) is made. It is clear from Eq. (A.10) that α is proportional to $i\langle A \rangle$ in Eq. (A.18).

-
- [1] W. Zhang, C. A. Sackett, and R. G. Hulet, *Phys. Rev. A* **60**, 504 (1999); F. Weig and W. Zwerger, *Europhys. Lett.* **49**, 282 (2000).
- [2] E. Altman, E. Demler, and M. D. Lukin, *Phys. Rev. A* **70**, 013603 (2004).
- [3] J. Ruostekoski, *Phys. Rev. A* **61**, 033605 (2000); A. Minguzzi, G. Ferrari, and Y. Castin, *Eur. Phys. J. D* **17**, 49 (2001); C. P. Search, H. Pu, W. Zhang, and P. Meystre, *Phys. Rev. Lett.* **88**, 110401 (2002).
- [4] R. Combescot, S. Giorgini, and S. Stringari, *Europhys. Lett.* **75**, 695 (2006); G. Veeravalli, E. Kuhnle, P. Dyke, and C. J. Vale, *Phys. Rev. Lett.* **101**, 250403 (2008).
- [5] P. Törmä and P. Zoller, *Phys. Rev. Lett.* **85**, 487 (2000); G. M. Bruun, P. Törmä, M. Rodriguez, and P. Zoller, *Phys. Rev. A* **64**, 033609 (2001).
- [6] G. M. Bruun and G. Baym, *Phys. Rev. Lett.* **93**, 150403 (2004).
- [7] C. Chin, M. Bartenstein, A. Altmeyer, S. Riedl, S. Jochim, J. Hecker Denschlag, and R. Grimm, *Science* **305**, 1128 (2004).
- [8] J. Kinnunen, M. Rodriguez, and P. Törmä, *Science* **305**, 1131 (2004); *Phys. Rev. Lett.* **92**, 230403 (2004).
- [9] J. Ruostekoski, *Phys. Rev. A* **60**, R1775 (1999).
- [10] I. Carusotto and Y. Castin, *Phys. Rev. Lett.* **94**, 223202 (2005).
- [11] C. A. Regal and D. S. Jin, *Phys. Rev. Lett.* **90**, 230404 (2003).
- [12] S. Gupta, Z. Hadzibabic, M. W. Zwierlein, C. A. Stan, K. Dieckmann, C. H. Schunck, E. G. M. van Kempen, B. J. Verhaar, and W. Ketterle, *Science* **300**, 1723 (2003).
- [13] K.-J. Boller, A. Imamoglu, and S. E. Harris, *Phys. Rev. Lett.* **66**, 2593 (1991); M. Xiao, Y. Q. Li, S. Z. Jin, and J. Gea-Banaclache, *ibid.* **74**, 666 (1995).
- [14] E. Arimondo, in *Progress in Optics XXXV*, edited by E. Wolf (Elsevier, Amsterdam, 1996), p. 257.
- [15] L. V. Hau, S. E. Harris, Z. Dutton, and C. H. Behroozi, *Nature (London)* **397**, 594 (1999); M. M. Kash, V. A. Sautenkov, A. S. Zibrov, L. Hollberg, G. R. Welch, M. D. Lukin, Y. Rostovtsev, E. S. Fry, and M. O. Scully, *Phys. Rev. Lett.* **82**, 5229 (1999).
- [16] R. W. Boyd and D. J. Gauthier, in *Progress in Optics*, edited by E. Wolf (Elsevier, Amsterdam, 2002), Vol. 43, p. 497.
- [17] M. Fleischhauer and M. D. Lukin, *Phys. Rev. Lett.* **84**, 5094 (2000); C. Liu, Z. Dutton, C. Behroozi, and L. V. Hau, *Nature (London)* **409**, 490 (2001).
- [18] K. J. Weatherill, J. D. Pritchard, R. P. Abel, M. G. Bason, A. K. Mohapatra, and C. S. Adams, *J. Phys. B* **41**, 201002 (2008).
- [19] Y. He, Q. Chen, and K. Levin, *Phys. Rev. A* **72**, 011602(R) (2005); Q. Chen, J. Stajic, S. Tan, and K. Levin, *Phys. Rep.* **412**, 1 (2005).
- [20] Y. Ohashi and A. Griffin, *Phys. Rev. A* **72**, 013601 (2005).
- [21] Z. Yu and G. Baym, *Phys. Rev. A* **73**, 063601 (2006).
- [22] A. Perali, P. Pieri, and G. C. Strinati, *Phys. Rev. Lett.* **100**, 010402 (2008).
- [23] S. Basu and E. J. Mueller, *Phys. Rev. Lett.* **101**, 060405 (2008).
- [24] C. Schunck, Y. Shin, A. Schirotzek, M. W. Zwierlein, and W. Ketterle, *Science* **316**, 867 (2007).
- [25] Y. He, C. C. Chien, Q. Chen, and K. Levin, *Phys. Rev. A* **77**, 011602(R) (2008).
- [26] P. Massignan, G. M. Bruun, and H. T. C. Stoof, *Phys. Rev. A* **77**, 031601(R) (2008).
- [27] Y. Shin, C. H. Schunck, A. Schirotzek, and W. Ketterle, *Phys. Rev. Lett.* **99**, 090403 (2007).
- [28] A. Schirotzek, Y. I. Shin, C. H. Schunck, and W. Ketterle, *Phys. Rev. Lett.* **101**, 140403 (2008).
- [29] M. W. Zwierlein, A. Schirotzek, C. H. Schunck, and W. Ketterle, *Science* **311**, 492 (2006); G. B. Partridge, W. Li, R. I. Kamar, Y. Liao, and R. G. Hulet, *ibid.* **311**, 503 (2006).
- [30] C. H. Schunck, Y. Shin, A. Schirotzek, and W. Ketterle, *Nature (London)* **454**, 739 (2008).
- [31] H. Y. Ling, Y.-Q. Li, and M. Xiao, *Phys. Rev. A* **53**, 1014 (1996).
- [32] J. T. Stewart, J. P. Gaebler, and D. S. Jin, *Nature (London)* **454**, 744 (2008).
- [33] G. D. Mahan, *Many-Particle Physics* (Indiana University Press, Bloomington, IN, 1980).